Am J Cancer Res 2025;15(2):452-469
www.ajcr.us /ISSN:2156-6976/ajcr0159225

Original Article

GDF15 promotes the resistance of epithelial ovarian cancer cells to gemcitabine via DHCR24-mediated cholesterol metabolism to elevate ABCB1 and ABCC1 levels in lipid rafts

Linlin Guo[1], Yan He[2], Huang Xin[1]

[1]*Department of Obstetrics and Gynecology, First Affiliated Hospital of Jinzhou Medical University, No. 2, Section 5, Renmin Street, Guta District, Jinzhou 121001, Liaoning, PR China;* [2]*Department of Laboratory, Animal Science, China Medical University, No. 77 Puhe Road, Shenyang North New Area, Shenyang 110122, Liaoning, PR China*

Received July 16, 2024; Accepted February 6, 2025; Epub February 15, 2025; Published February 28, 2025

Abstract: Growth differentiation factor 15 (GDF15) is upregulated in most cases of epithelial ovarian cancer (EOC); however, its functions in EOC are not fully understood. In this study, we knocked down GDF15 in EOC cells before performing high-throughput sequencing to identify genes regulated by GDF15. GDF15 was overexpressed to determine its effect on the viability, migration, and response of EOC cells to gemcitabine, carboplatin, and paclitaxel. Reprogramming of glucose and cholesterol metabolism in EOC cells was evaluated based on oxygen consumption, lactic acid production, complex I activity, and free and esterified cholesterol levels. The activities of ATP-binding cassette (ABC)B1 and ABCC1 were assessed based on the expulsion efficiency of rhodamine 12. GDF15 overexpression promoted cell viability, migration, and resistance to gemcitabine. In addition, GDF15 induced glycolysis and increased cholesterol levels in EOC cells. Cholesterol metabolism regulated by GDF15 contributed to the resistance of EOC cells to gemcitabine by elevating ABCB1 and ABCC1 levels in lipid rafts. DHCR24 plays an important role in cholesterol synthesis. DHCR24 was identified as a downstream effector of GDF15, because knockdown of DHCR24, but not treatment with statins, suppressed the cancer-promoting effect of GDF15. Overall, GDF15 promoted the resistance of EOC cells to gemcitabine via DHCR24-mediated cholesterol metabolism to elevate ABCB1 and ABCC1 levels in lipid rafts. Therefore, GDF15 and DHCR24 are potential therapeutic targets for suppressing the growth of EOC cells and improving their sensitivity to gemcitabine.

Keywords: GDF15, epithelial ovarian cancer, gemcitabine, DHCR24, cholesterol metabolism, lipid raft, statin

Introduction

Ovarian cancer continues to pose a serious health threat as one of the most significant female malignant tumors. Recent data shows over 50000 new cases of ovarian cancer and over 20000 deaths in China annually [1, 2]. The early symptoms of ovarian cancer are relatively concealed, leading to its diagnosis at a late stage in many patients, greatly increasing the challenge of treatment. The current standard treatment strategy for early stage ovarian cancer is still dominated by surgery and postoperative chemotherapy. For patients at a late stage, chemotherapy has become one of the few available options for controlling the progression of ovarian cancer. However, many challenges are associated with chemotherapy, such as drug resistance and toxic side effects, which seriously affect the clinical prognosis of patients. The overall five-year survival rate of ovarian cancer patients below 50% is still unsatisfactory [1, 2].

Epithelial ovarian cancer (EOC) is the main subtype of ovarian cancer, accounting for approximately 70% of all ovarian cancer cases. EOC cells exhibit an aggressive proliferation pattern, partly because the energy metabolism of most EOC cells undergoes reprogramming. In addition, metabolic reprogramming helps EOC cells adapt to different tumor microenvironments.

https://doi.org/10.62347/KYIY8286

During the occurrence and development of tumors, the energy metabolism pattern of cells undergoes significant changes to cope with the metabolic pressure in the microenvironment at different stages [3]. The role of cholesterol metabolism in EOC has received increasing attention. Reprogramming of cholesterol metabolism pathways is considered a marker of EOC progression [4]. Recent studies have shown that targeting cholesterol metabolism can inhibit the proliferation and invasion of EOC cells and attenuate drug resistance [5]. Therefore, the development of anti-tumor drugs with cholesterol inhibition has important clinical significance for the treatment of EOC.

Lipid rafts are heterogeneous and highly fluid, ranging from 10 to 200 nm in the cell membrane. They are rich in cholesterol and provide a platform for proteins and lipids to regulate their biological activities. A variety of membrane receptors (e.g., epidermal growth factor receptor) and transport proteins, such as ATP-binding cassette (ABC) transporter family members, are concentrated in lipid rafts [6]. ABC transporter superfamily members participate in the transport of a wide range of lipophilic and amphiphilic compounds in an ATP-dependent manner. Some family members, such as ABCB1 (also known as MDR-1 and P-gp), ABCC1 (also known as MRP-1), and ABCG2, are upregulated in cancers and are associated with multidrug resistance [7, 8]. ABCB1 expels a broad range of anticancer drugs from cells and is implicated in both intrinsic and acquired drug resistance [7, 8].

Growth differentiation factor 15 (GDF15) is a member of the transforming growth factor β superfamily. GDF15 can bind to its receptor, GDNF family receptor alpha like (GFRAL), and then induce RET to activate the downstream AKT and MAPK signaling pathways [8, 9]. Therefore, GDF15 plays an important role in pathological processes such as proliferation, invasion, and drug resistance in EOC cells. Immunohistochemical studies have found that GDF15 levels in ovarian cancer tissues are closely related to matrix metallopeptidase 2 and 9, indicating that GDF15 levels are closely related to EOC metastasis and migration [9, 10]. Our previous study also found high expression of GDF15 in EOC cells, which was induced by the downregulation of the long noncoding RNA GAS5 through CCAAT enhancer-binding protein beta. High GDF15 expression promotes cancer cell proliferation and invasion by suppressing apoptosis [11]. Using high-throughput sequencing, this study revealed, for the first time, more unreported genes regulated by GDF15 in EOC cells. This study aimed to explore a new pathological mechanism of action of GDF15 in EOC.

Materials and methods

Bioinformatics analysis

GDF15 mRNA expression and protein levels were analyzed in ovarian cancer and corresponding normal tissues using data from the TCGA database (http://gepia.cancer-pku.cn/index.html) and UALCAN (https://ualcan.path.uab.edu/analysis-prot.html), respectively. UALCAN provides protein expression analyses using data from the Clinical Proteomic Tumor Analysis Consortium and International Cancer Proteogenome Consortium datasets. The association of GDF15 expression with the overall survival of patients with ovarian cancer was analyzed using hazard ratio using OSov, a public website for bioinformatics analysis (https://bioinfo.henu.edu.cn/OV/OVList.jsp). OSov encompasses 22 expression datasets containing information on 3238 patients with ovarian cancer.

Cell culture

The OC cell lines OVCAR3 and SKOV3 were obtained from the American Type Culture Collection (Rockville). SKOV3 cells were cultured in Dulbecco's Modified Eagle's medium (DMEM; Gibco, China) supplemented with 10% fetal bovine serum (FBS; Gibco). OVCAR3 cells were maintained in RPMI-1640 medium (Gibco) supplemented with 10% FBS. Cell cultivation was performed in a humidified 5% CO_2 and 37°C incubator, and the culture medium was replaced three times each week.

Cell transfection

Short hairpin (sh)RNAs targeting GDF15 and DHCR24 and the corresponding negative control were synthesized by GenePharma (Suzhou, China) to induce RNA knockdown. The shRNA sequences used in this study are listed in **Table 1**. A full-length complementary DNA (cDNA) of

Table 1. The information of shRNAs

Gene	Numb.	Sequences (5'-3')
GDF15	1	AGACTCCAGATTCCGAGAGTT
	2	GCTCCAGACCTATGATGACTT
	3	TCTCAGATGCTCCTGGTGTTG
DHCR24	1	GCTCTCGCTTATCTTCGATAT
	2	GCTCTCGCTTATCTTCGATAT
	3	CGAGTCATCATCCCACAAGTA

human GDF15 was synthesized by Sangon Biotech and cloned into the pcDNA3.1 vector (TAKARA, Beijing, China) to construct the overexpression plasmid pcDNA-GDF15. A DNA Midiprep Kit (Thermo Fisher Scientific) was used to prepare the overexpression plasmid. OVCAR3 and SKOV3 cells were plated in 6-well plates (2×10^5/well) and grown in a 37°C incubator overnight. Transfection was performed using Lipofectamine 3000 (Invitrogen-California). Cells were harvested 48 h post transfection for further experiments. Transduction of OVCAR3 cells with a lentivirus-encapsulated GDF15 overexpression vector and DHCR24 shRNA resulted in stable overexpression of GDF15 and knockdown of DHCR24.

Quantitative reverse-transcription polymerase chain reaction (qRT-PCR)

RNA was isolated using TRIZOL reagent (TAKARA). Reverse transcription was performed using oligo(dT) primers and Revertaid M Mulv Reverse Transcriptase (Thermo Fisher Scientific). Thereafter, qRT-PCR was performed using 2×SYBR Green PCR Master mix (Thermo Fisher Scientific) using the $2^{-\Delta\Delta Ct}$ method. The primers used in this study are listed in **Table 2**.

Western blot

Proteins were extracted using RIPA lysis buffer (Beyotime, Shanghai, China) in the presence of protease inhibitors (Thermo Fisher Scientific). Proteins were separated by SDS-PAGE and transferred onto nitrocellulose membranes. Primary antibodies were used to target the indicated proteins on the membranes. Detailed information regarding the primary antibodies used is provided in **Table 3**. The targeted proteins were observed by incubation with an HRP-labeled secondary antibody (ab6721, Abcam) and ECL reagent using the LAS-3000 (FUJIFILM, Tokyo, Japan) system.

Cell viability test

The 3-[4,5-Dimethylthiazol-2-yl]-2,5-diphenyltetrazoliumbromide (MTT) was used to assess cell viability. Briefly, 50 µl of MTT reagent was dissolved in PBS and added to each well of a 96-well plate in a 37°C incubator. Thereafter, 150 µl of dimethyl sulfoxide was added to each well to dissolve formazan. Optical density was measured at 570 nm using a microplate reader (Bio-Rad, Hercules, CA).

Apoptosis test

Cells were incubated with Annexin V-FITC and propidium iodide (PI) and analyzed by flow cytometry using FlowJo software. After fluorescence analysis, the software generated a scatter plot, and the areas of Annexin V+/PI+ and Annexin V+/PI- were regarded as apoptotic cells.

Cell migration test

Cells were seeded in 6-well plates and grown to approximately 90% confluence. Cells were scraped with a pipette and rinsed with serum-free 10% FBS medium for 24 h. To exclude the interference of cell proliferation in cell migration, we added the cell division inhibitor mitomycin (1 µg/ml, Selleck). Cell migration was examined using phase-contrast microscopy (Olympus, Tokyo, Japan).

Co-immunoprecipitation

Cells were incubated with RIPA lysis buffer (Beyotime) in the presence of protease inhibitors (Thermo Fisher Scientific). Cell lysate supernatants were incubated with primary anti-GFRAL antibody or control IgG at 4°C overnight. Protein A/G PLUS-agarose beads (Santa Cruz Biotechnology) were mixed with the cell lysates at 4°C for 2 h. Thereafter, the beads were isolated for RET analysis in the protein complex by western blotting.

Cholesterol measurement

The cellular free cholesterol concentration was measured using a cholesterol assay kit according to the manufacturer's instructions (ab-65390, Abcam). Briefly, cells were lysed and incubated with cholesterol oxidase. Fluorescence (Ex/Em=538/587 nm) was measured

Table 2. The information of Primer in PCR assay

Genes	Direction	Sequence (5'-3')	Tm
GDF15	Forward	GACCCTCAGAGTTGCACTCC	61.9
	Reverse	GCCTGGTTAGCAGGTCCTC	61.7
DHCR24	Forward	GCCGCTCTCGCTTATCTTCG	63
	Reverse	GTCTTGCTACCCTGCTCCTT	61.3
GAPDH	Forward	GGAGCGAGATCCCTCCAAAAT	61.6
	Reverse	GGCTGTTGTCATACTTCTCATGG	60.9

Table 3. The information of primary anti-bodies

Primary antibodies	MW (kDa)	Dilution	Company/Catalog
GDF15	34	1:100	Abcam/ab206414
DHCR24	50	1:100	Proteintech/10471-1-AP
GFRAL	44	1:100	NOVUS/NBP3-09606
RET	124	1:100	Abcam/ab134100
p-AKT	56	1:200	Abcam/ab38449
AKT	56	1:200	Abcam/ab8805
NPC1	149	1:100	Proteintech/13926-1-AP
NPC2	17	1:100	Proteintech/19888-1-AP
ABCB1	150	1:100	Proteintech/22336-1-AP
ABCC1	150	1:100	Proteintech/67228-1-Ig
p-ATM	351	1:200	Abcam/ab81292
ATM	351	1:200	Abcam/ab32420
FLOT1	48	1:100	Abcam/ab78178
CAV1	25	1:100	Proteintech/16447-1-AP
Histone3	15	1:500	Abcam/ab176842
GAPDH	40	1:500	Abcam/ab8245

using an Infinite F500 microplate reader (TECAN, Männedorf, Switzerland). Cholesteryl esters were tested by initially converting them into free cholesterol by cholesterol esterase. The total cholesterol was defined as the amount of free cholesterol and cholesterol esters.

Measurement of cell oxygen consumption rate

The cell oxygen consumption rate was measured using an oxygen consumption assay kit (Cayman Chemical, Ann Arbor, MI). Briefly, cells were treated with MitoXpress-Xtra for the indicated times, with mineral oil overlaid in each well. Finally, MitoXpress-Xtra fluorescence was detected using an Infinite F500 microplate reader (TECAN).

Measurement of glucose concentration in culture medium

He glucose concentration in the culture medium was determined using glucose oxidase/peroxidase method, which is based on the reaction that glucose oxidase converts glucose and O_2 into gluconic acid and H_2O_2. H_2O_2 further reacts with 1,5-dimethyl-2-phenyl-4-aminopyrazoline and phenols to generate colored compounds with a maximum absorption wavelength of 570 nm.

Intracellular lactic acid concentration measurement

Intracellular lactic acid concentration was determined using a lactic acid assay kit (Biovision, Wuhan, China) according to the manufacturer's instructions. The highly sensitive probe in the kit generated fluorescence (Ex/Em=535/587 nm) after reaction with lactic acid. Fluorescence was detected using an Infinite F500 microplate reader (TECAN).

Extracellular medium acidification rate (ECAR) measurement

Cells were seeded in 24-well plates at 2.5×10^4 cells/well. Before the measurements, the medium was replaced with 500 μL of DMEM containing 10 mmol/L D-glucose and 2 mmol/L L-glutamine. After steady-state extracellular acidification rates were obtained, the ATP synthase inhibitor oligomycin (5 μM) was added to observe changes after blocking mitochondrial respiration. Finally, 2-deoxyglucose (100 mM) was added to suppress glycolysis.

Complex I activity test

Mitochondrial respiratory chain complex I activity was detected using a SolarBio detection kit (BC0510; Beijing, China). Briefly, the collected cells were mixed with the reagents supplied by the manufacturer before measuring the absorbance of each sample at 340 nm. One unit of enzyme activity was defined as the amount of enzyme catalyzing the consumption of 1 nmol NADH per minute per milligram of protein.

Lipid raft isolation

Cells were washed with a base buffer (20 mM Tris-HCl, pH7.8, 250 mM sucrose) supplement-

ed with 1 mM $CaCl_2$, 1 mM $MgCl_2$, and protease inhibitors. Cells were then lysed by passage through a 22 gauge ×3 needle 20 times. The lysates were centrifuged at 1,000×g for 10 min. An equal volume (2 ml) of base buffer containing 50% OptiPrep (Axis-Shield, 12ICS06) was added to the supernatant, followed by centrifugation for 90 min at 22,000 rpm at 4°C.

Measurement of rhodamine 123 (R123) efflux

Cells were incubated with R123 (10 μM in HBSS) at 10°C for 60 min. After washing with ice-cold HBSS, cells were cultured at 37°C for different time periods. The efflux of R123 was stopped by mixing the cells with ice-cold HBSS containing cyclosporin A (10 μM at final concentration). The remaining R123 in the cells was determined by measuring fluorescence using an Infinite F500 microplate reader (TECAN).

Animal study

Twenty-four female BALB/c-nu nude mice (aged 4-6 weeks) were acquired from the Experimental Animal Center of China Medical University (China). All animal experiments were approved by the Ethics Committee for Animal Research of Jinzhou Medical University (approval number: 240106). The mice were divided into eight groups, with three mice per group. OVCAR3 cells in the control group and those with stable GDF15 overexpression and DHCR24 knockdown were injected subcutaneously into nude mice. Nude mice with GDF15-overexpressed OVCAR3 cells were orally administered mevastatin (500 mg/kg) every 2 days to inhibit cholesterol levels in the blood. Half of the mice were intraperitoneally administered gemcitabine (100 mg/kg) once a week. Normal saline was administered to the other half. Tumor volume was calculated according to the following formula: tumor volume (V, mm^3) = 0.5 × length × width. Mice were sacrificed using the cervical dislocation method. Tumor tissues were collected for western blot analysis.

Measurement of GDF15 in cell culture medium and tumor interstitial fluid

Human GDF15 Elisa Detection Kit was obtained from Abcam (ab155432). The concentration of GDF15 was tested in the culture medium of OVCAR3 and SKOV3 cells using the detection kit according to the manufacturer's instructions. The interstitial fluid in xenograft tumors was obtained using a previously reported method [12]. Briefly, xenograft tumor tissues were harvested, placed on a triple-layered 10 μM nylon mesh, and spun at <50×g for 5 min to remove surface liquid. Next, the samples were centrifuged at 400×g, a previously validated speed at which intracellular contents are not liberated, for an additional 10 min. The fluid from this step was retained as interstitial fluid. The concentration of GDF15 was also tested in the interstitial fluid using the detection kit.

Statistical analysis

Each experiment was performed in triplicates. Data analysis was performed using GraphPad Prism software (GraphPad Software, CA). Data were expressed as mean ± standard deviation. Comparisons between two groups and among multiple groups were conducted using Student's *t*-test and one-way ANOVA, followed by Tukey's post hoc test. $P<0.05$ was considered statistically significant.

Results

Upregulation of GDF15 in ovarian cancer

As indicated by the TCGA database, GDF15 expression was upregulated in ovarian cancer tissues compared with that in the corresponding normal tissues (Supplementary Figure 1A). In addition, our previous study confirmed the upregulation of GDF15 mRNA and protein expression in EOC cells [11]. Data from the TCGA database showed that GDF15 mRNA expression was marginally increased in patients with ovarian cancer aged 61-80 years compared with that in patients at other age stages (Supplementary Figure 1B). Data from UALCAN showed that GDF15 protein levels were significantly increased in ovarian cancer patients aged 61-80 years compared with those aged 40-60 years (Supplementary Figure 1C). As indicated by the TCGA database, GDF15 expression levels were not related to the prognosis of patients with ovarian cancer (Supplementary Figure 1D). However, OSov showed that GDF15 expression was related to the overall survival of patients with ovarian cancer according to data from the GSE53963, GSE49997, GSE3149, GSE8841, and GSE18520 datasets (Supplementary Figure 1E). Age, stage, histology, and grade, but not GDF15 expression, were

related to the overall survival of patients with ovarian cancer in several univariate and multivariate analyses using data from the GSE51088, GSE73614, and GSE9891 datasets (Supplementary Figure 1F).

High-throughput sequencing revealed genes regulated by GDF15 in EOC cells

Since the effect of GDF15 on EOC cells is not completely understood, we initially conducted high-throughput sequencing after GDF15 knockdown to identify genes regulated by GDF15 in EOC cells. Three shRNAs targeting GDF15 were transfected into EOC, OVCAR3, and SKOV3 cells. As indicated by both PCR and western blot assays, shRNA3 showed the strongest effect on the knockdown of GDF15 among all the shRNAs (**Figure 1A** and **1B**). shRNA2 exerted the second strongest effect on the knockdown of GDF15, followed by shRNA1. All three shRNAs were individually transfected into OVCAR3 and SKOV3 cells before high-throughput sequencing to exclude interference caused by the different efficiencies in the knockdown of GDF15 by the three shRNAs. **Figure 1C** and **1D** show the heatmap and principal component analysis picture, respectively. A Venn diagram was used to identify the same downregulated genes after transfection with the three shRNAs. As shown in **Figure 1E**, 429 genes were downregulated by all the three shRNAs in OVCAR3 cells. In addition, 696 genes were downregulated by all the three shRNAs in SKOV3 cells. In total, 291 genes were downregulated by all the three shRNAs in both OVCAR3 and SKOV3 cells. Using the same method, we identified 437 genes that were upregulated by all the three shRNAs in both OVCAR3 and SKOV3 cells (**Figure 1F**).

GDF15 induced GFRAL/RET/AKT signalling in EOC cells

In theory, upon binding to extracellular GDF15, GFRAL interacts with RET and activates the AKT signaling pathway [13]. We previously confirmed that EOC cells express GDF15 [11], but it is unclear whether GDF15 can be secreted by EOC cells to activate GFRAL/RET/AKT signaling in EOC cells. Since AKT is a well-known pro-cancer signal, identifying the self-activating signal of GDF15 in EOC cells is important. OVCAR3 and SKOV3 cells were transfected with a GDF15 expression vector. Both PCR and western blotting confirmed the upregulation of GDF15 in OVCAR3 and SKOV3 cells after transfection with the GDF15 expression vector (**Figure 2A** and **2B**). More importantly, we detected an increase in GDF15 levels in the cell culture medium after transfection with the GDF15 expression vector, using a GDF15 ELISA detection kit. GDF15 expression decreased in the culture medium after cells were transfected with shRNA2 and shRNA3. These results suggested that the secreted level of GDF15 was positively correlated with GDF15 expression levels in EOC cells (**Figure 2C**). Co-immunoprecipitation assays were performed to confirm the interaction between GFRAL and RET in EOC cells. GDF15 knockdown using shRNA2 and shRNA3 reduced RET enrichment in GFRAL cells (**Figure 2D**). Conversely, overexpression of GDF15 increased RET enrichment in GFRAL cells. Western blotting indicated that the total protein levels of GFRAL and RET were not influenced by the knockdown and overexpression of GDF15. As an important downstream effector of RET, AKT showed decreased and increased phosphorylation after the knockdown and overexpression of GDF15, respectively. These results confirmed the activation of GFRAL/RET/AKT signaling in EOC cells by the secreted GDF15.

GDF15 increased cholesterol levels and induced glycolysis in EOC cells

High-throughput sequencing assays showed that the expression of many genes was affected by GDF15 knockdown. Downregulated genes were used for GO enrichment analysis to determine the biological processes regulated by GDF15. This analysis implied that metabolic pathways, such as cholesterol and glycolysis, are regulated by GDF15 (Supplementary Figure 2). Free cholesterol and total cholesterol, but not cholesterol esters, decreased after transfection with shRNA2 and shRNA3 knockdown of GDF15 (**Figure 3A**). Conversely, overexpression of GDF15 increased free cholesterol and total cholesterol levels in EOC cells (**Figure 3B**). DHCR24, NPC1, and NPC2 are implicated in cholesterol biosynthesis and uptake. They were found to be regulated by GDF15 according to the results of the high-throughput sequencing assay. Western blotting was performed to confirm these results. As shown in **Figure 3C**, DHCR24 protein levels were decreased by

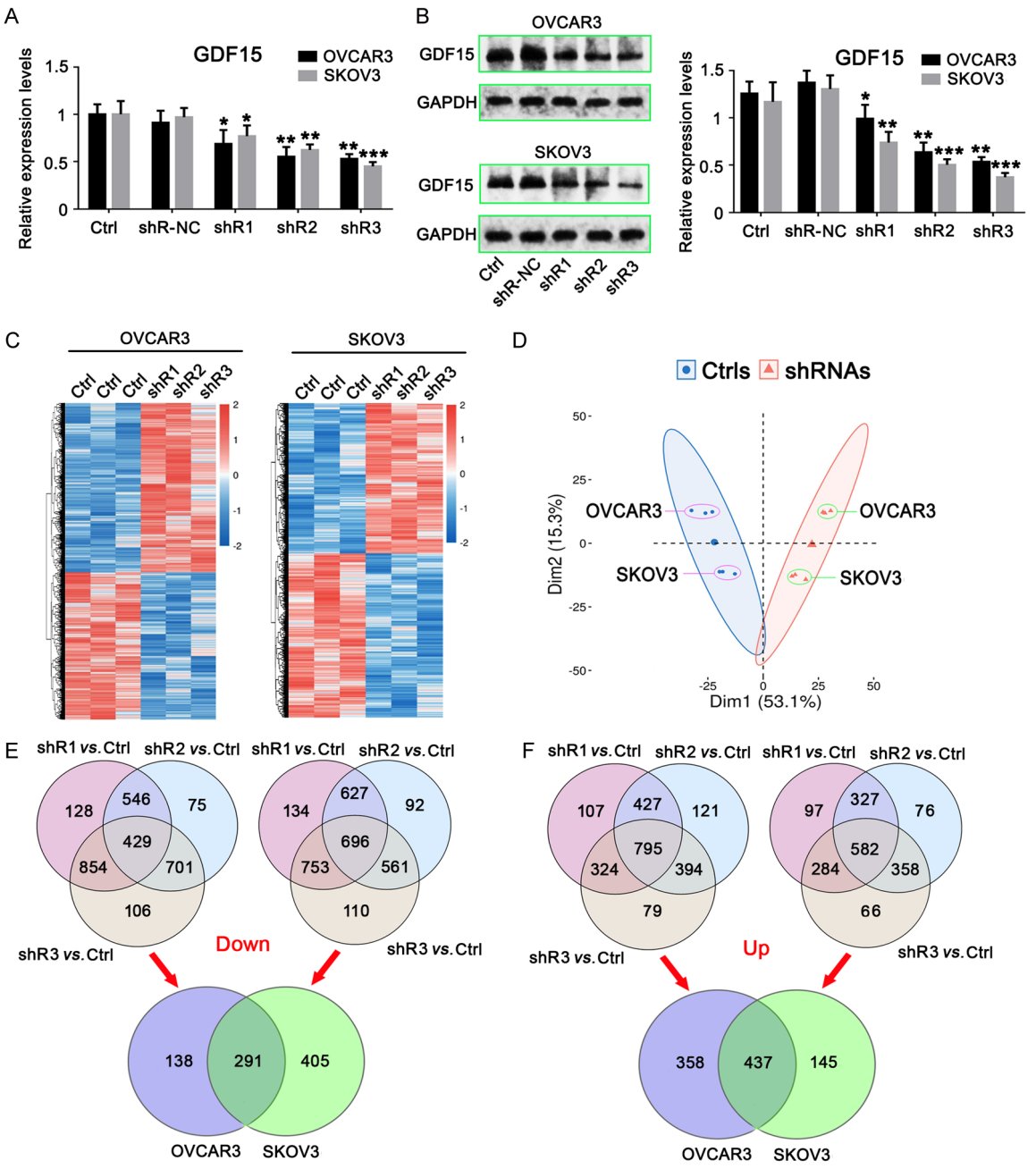

Figure 1. High-throughput sequencing revealed genes regulated by GDF15 in EOC. Three shRNAs targeting GDF15 were transfected to EOC OVCAR3 and SKOV3 cells. (A) PCR and (B) western blot assays were conducted to test the mRNA and protein level of GDF15, respectively. (C) All the three shRNAs have been individually transfected to OVCAR3 and SKOV3 cells before the high-throughput sequencing assay. (D) The principal component analysis (PCA). (E) Venn diagram was used to find the same down-regulated genes after the transfection of the three shRNAs. (F) Venn diagram was used to find the same up-regulated genes after the transfection of the three shRNAs. Data expressed as mean ± standard deviation. *P*-value <0.05 was defined as specific statistical significance (*P<0.05, **P<0.01, ***P<0.001).

GDF15 knockdown but increased by GDF15 overexpression. Although NPC1 and NPC2 were also regulated by GDF15, their regulatory effects were much weaker than those of DHCR24.

The oxygen consumption test showed that GDF15 knockdown by shRNA3 increased oxygen consumption, whereas GDF15 overexpression decreased it (**Figure 3D**). GDF15 knock-

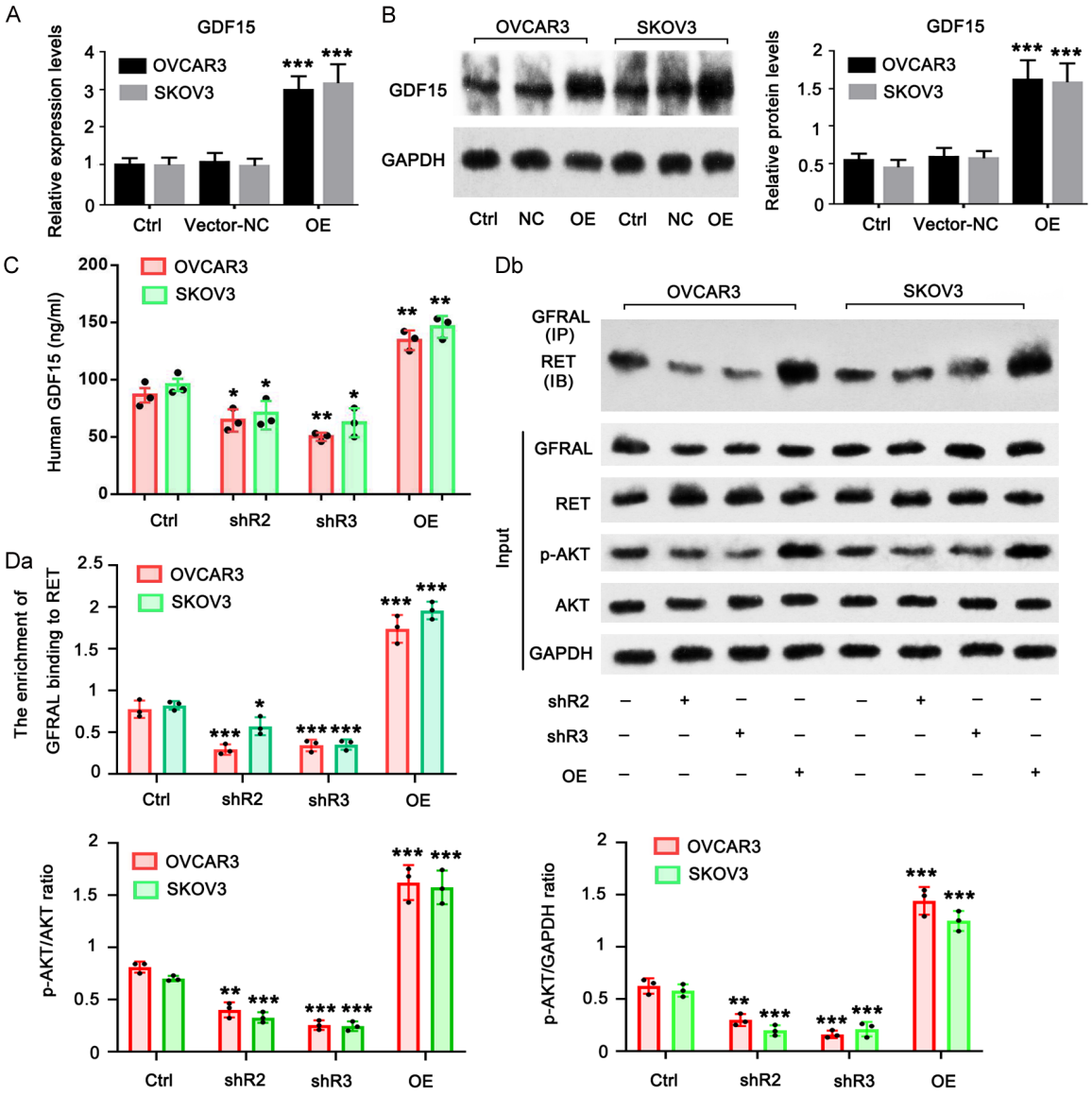

Figure 2. GDF15 induces the GFRAL/RET/AKT signal in EOC. OVCAR3 and SKOV3 cells were transfected with GDF15 expression vector. (A) PCR, (B) western blot and (C) Elisa assays were conducted to test the mRNA and protein level of GDF15 as well as the secreted GDF15. (D) Co-IP assay was undertaken to confirmed the interaction between GFRAL and RET in EOC. Data expressed as mean ± standard deviation. *P*-value <0.05 was defined as specific statistical significance (*P<0.05, **P<0.01, ***P<0.001).

down decreased glucose consumption and intracellular lactic acid levels (**Figure 3E** and **3G**). GDF15 overexpression increased glucose consumption and intracellular lactic acid levels but inhibited complex I activity (**Figure 3E-G**). This study also tested the ECAR to assess lactic acid secreted by EOC cells. GDF15 knockdown decreased the ECAR, whereas GDF15 overexpression increased it (Supplementary Figure 3). These results indicated that GDF15 induces glycolysis in EOC cells.

GDF15 suppressed the toxicity of gemcitabine in EOC cells

OVCAR3 and SKOV3 cells were exposed to different doses of carboplatin, gemcitabine, and paclitaxel, the three chemotherapeutic drugs used in ovarian cancer. Carboplatin, gemcitabine, and paclitaxel decreased the viability of OVCAR3 and SKOV3 cells in a dose-dependent manner (**Figure 4A-C**). The IC50 of gemcitabine was 2.32 and 2.41 μM in OVCAR3 and

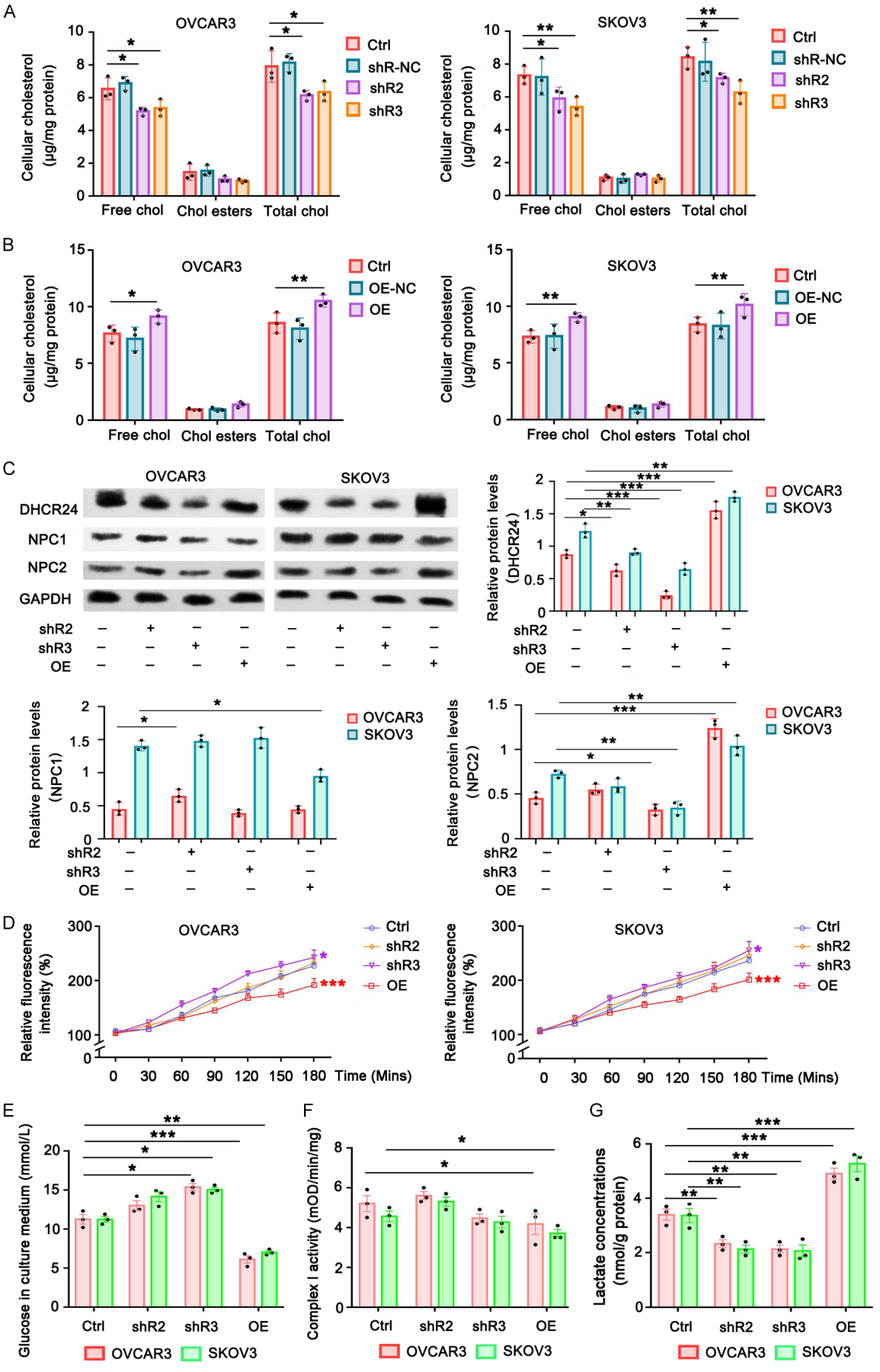
A
OVCAR3
SKOV3
Cellular cholesterol (μg/mg protein)
Free chol
Chol esters
Total chol
Ctrl
shR-NC
shR2
shR3
B
OE-NC
OE
C
DHCR24
NPC1
NPC2
GAPDH
Relative protein levels (DHCR24)
Relative protein levels (NPC1)
Relative protein levels (NPC2)
D
Relative fluorescence intensity (%)
Time (Mins)
E
Glucose in culture medium (mmol/L)
F
Complex I activity (mOD/min/mg)
G
Lactate concentrations (nmol/g protein)

Figure 3. GDF15 increased the cholesterol and induced glycolysis in EOC. (A) The free cholesterol, ester cholesterol and total cholesterol in EOC after the transfection with the shRNA2 and shRNA3 knocking down GDF15. (B) The free cholesterol, esterified cholesterol and total cholesterol in EOC after overexpressing GDF15. (C) Western blot was conducted to detect DHCR24, NPC1 and NPC2 protein levels after GDF15 knockdown and overexpression. (D) the oxygen consumption, (E) glucose level in culture medium, (F) the complex I activity and (G) lactic acid level in culture medium were tested after GDF15 knockdown and overexpression. Data expressed as mean ± standard deviation. *P*-value <0.05 was defined as specific statistical significance (*P<0.05, **P<0.01, ***P<0.001).

SKOV3 cells, respectively. The IC50 of carboplatin was 15.22 and 17.67 μM in OVCAR3 and SKOV3 cells, respectively. The IC50 of paclitaxel was 125.61 and 107.53 nM in OVCAR3 and SKOV3 cells, respectively. The drugs were classified into low, medium, and high doses based on their IC50 values. GDF15 overexpression further reduced the viability of OVCAR3 and SKOV3 cells upon treatment with low, medium, or high doses of gemcitabine. GDF15 overexpression further decreased the viability of SKOV3 cells at high carboplatin doses. GDF15 overexpression further reduced the viability of OVCAR3 cells upon treatment with high doses of paclitaxel, as well as with medium and high doses of paclitaxel. Thus, GDF15 more effectively suppressed the toxicity of gemcitabine than carboplatin and paclitaxel in EOC cells. We conducted apoptosis and cell migration assays to further investigate the protective effects of GDF15 against gemcitabine toxicity in EOC cells. Treatment with gemcitabine (5 μM) induced a significant increase in the apoptosis rate of EOC cells (**Figure 4D**). However, transfection of the GDF15 expression vector, but not of the negative control, suppressed the increase in the apoptosis rate of EOC cells upon gemcitabine treatment. The migratory capacity of EOC cells was also suppressed by gemcitabine (**Figure 4E**). GDF15 overexpression partially recovered the migratory capacity of EOC cells following gemcitabine treatment. To exclude the interference of cell proliferation in migration, we supplemented cells with mitomycin to suppress EOC cell proliferation. Similarly, gemcitabine suppressed the migratory capacity of EOC cells. GDF15 overexpression partially recovered the migratory capacity of EOC cells following gemcitabine treatment.

DHCR24 mediated the effect of GDF15 on the resistance of EOC cells to gemcitabine

Three shRNAs targeting DHCR24 were transfected into OVCAR3 and SKOV3 cells to knockdown DHCR24. As indicated by the PCR assay, shRNA1 showed the highest efficiency in decreasing DHCR24 expression in OVCAR3 and SKOV3 cells (**Figure 5A**). These results were confirmed by western blotting. shRNA1 showed the highest efficiency in the knockdown of DHCR24 protein (**Figure 5B**). shRNA1 was used for DHCR24 knockdown in the following study. Free cholesterol, esterified cholesterol, and total cholesterol were detected in OVCAR3 and SKOV3 cells. GDF15 overexpression increased free and total cholesterol in the cells, whereas DHCR24 knockdown reversed this increase (**Figure 5C**). Importantly, DHCR24 knockdown suppressed cell viability (**Figure 5D**) and increased the apoptotic rate of cells overexpressing GDF15 after gemcitabine treatment (**Figure 5E**). The migration of GDF15-overexpressed OVCAR3 and SKOV3 cells was suppressed by DHCR24 knockdown after gemcitabine treatment (**Figure 5F**). This effect was not influenced by the mitomycin-induced suppression of cell proliferation.

GDF15/DHCR24 increased ABCB1 and ABCC1 levels in lipid rafts to increase the resistance of EOC cells to gemcitabine

Cholesterol is the primary component of a lipid raft [14]. ABCB1 and ABCC1 in lipid rafts have been reported to have an enhanced ability to transport drugs outside cells [15]. Western blotting revealed that ABCB1 and ABCC1 levels increased with GDF15 overexpression in EOC cells exposed to gemcitabine or not, but DHCR24 knockdown suppressed the increase in ABCB1 and ABCC1 expression (**Figure 6A**). The ATM protein is sensitive to DNA damage caused by gemcitabine and initiates DNA repair. In the absence of gemcitabine, ATM phosphorylation was not affected by GDF15 overexpression or DHCR24 knockdown. Treatment with gemcitabine increased ATM phosphorylation, which was further enhanced by GDF15 overexpression. In this study, we isolated lipid rafts from EOC cells. FLOT1 and CAV1 are proteins located in a lipid raft [15]. FLOT1 and CAV1 were present in the isolated lipid raft but not in the remaining cell components (**Figure 6B**). His-

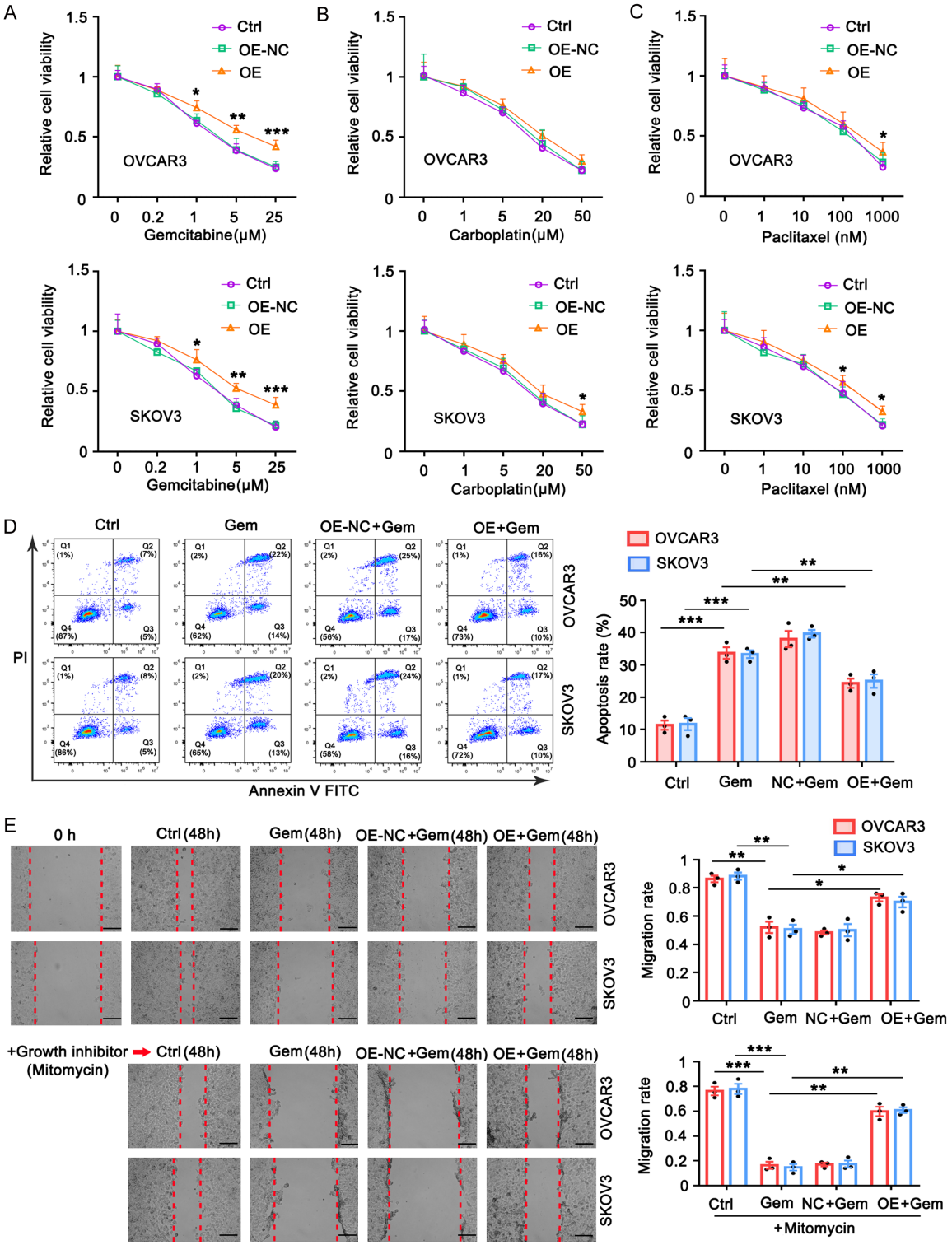

Figure 4. GDF15 suppressed the toxicity of Gemcitabine in EOC. OVCAR3 and SKOV3 cells were transfected with GDF15 expression vector or the negative control. A-C. OVCAR3 and SKOV3 cells were exposed to different dosages of Carboplatin, Gemcitabine and Paclitaxel, followed by test of the viability of OVCAR3 and SKOV3 cells. D. The apoptosis of OVCAR3 and SKOV3 cells after exposing to Gemcitabine (5 μM). E. Cell migration rate of OVCAR3 and SKOV3 cells after exposing to Gemcitabine (5 μM). The bar in the pictures indicates 100 μm. Data expressed as mean ± standard deviation. *P*-value <0.05 was defined as specific statistical significance (*P<0.05, **P<0.01, ***P<0.001).

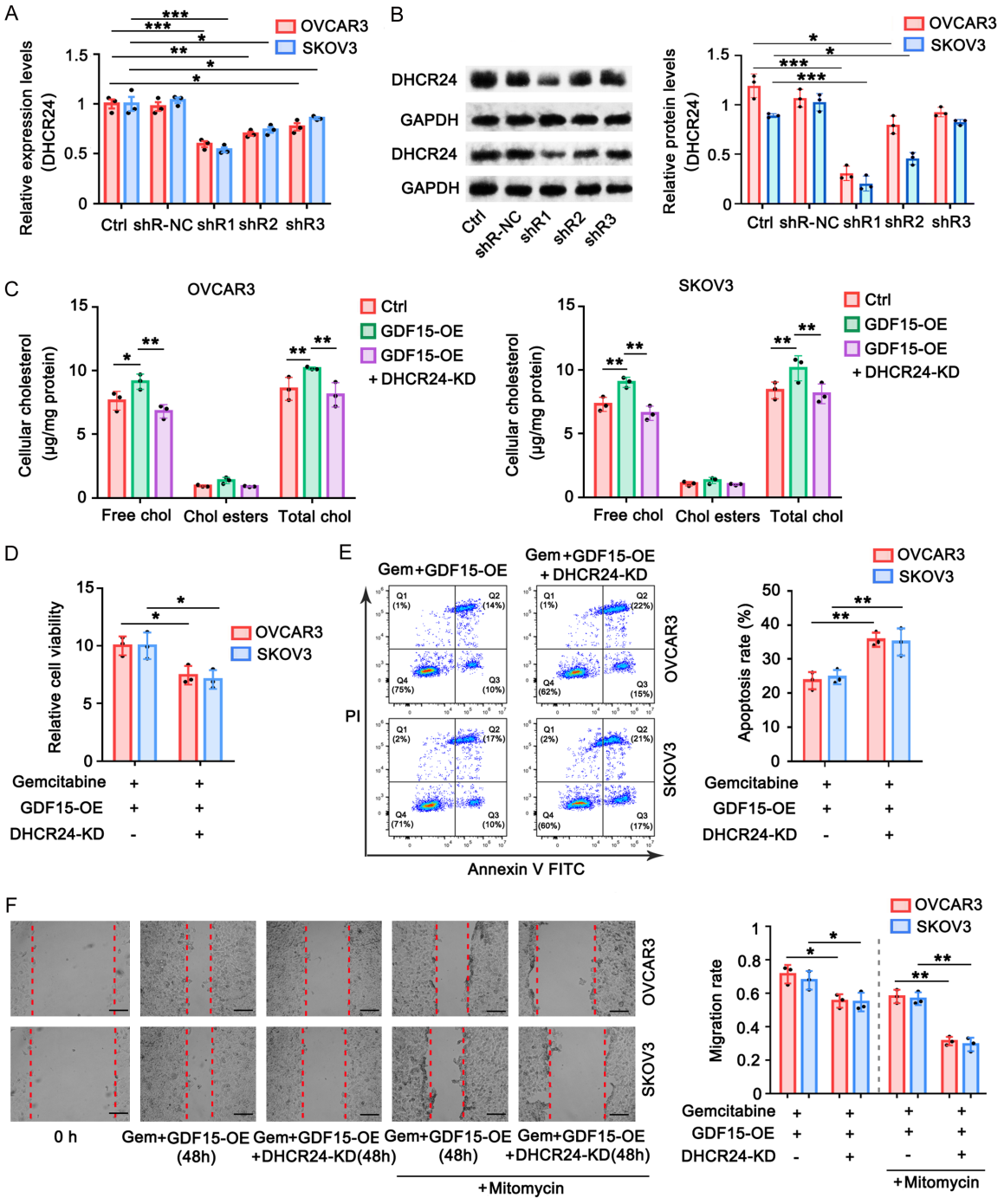

Figure 5. GDF15 increased cholesterol levels in EOC cells by DHCR24 thereby improving the resistance of EOC to Gemcitabine. Three kinds of shRNAs targeting DHCR24 were transfected to OVCAR3 and SKOV3 cells to knocked down DHCR24 in the cells. (A) PCR and (B) western blot assays were conducted to detect the mRNA and protein of DHCR24. (C) The free cholesterol, esterified cholesterol and total cholesterol in EOC after overexpressing GDF15 and knocking down DHCR24. (D) Cell viability, (E) apoptosis and (F) migration rate were tested after overexpressing GDF15 and knocking down DHCR24. The bar in the pictures indicates 100 μm. Data expressed as mean ± standard deviation. *P*-value <0.05 was defined as specific statistical significance (*P<0.05, **P<0.01, ***P<0.001).

tone3 and GAPDH are proteins located in the nucleus and cytoplasm, respectively. These proteins were not detected in the isolated lipid raft, suggesting successful isolation of the lipid

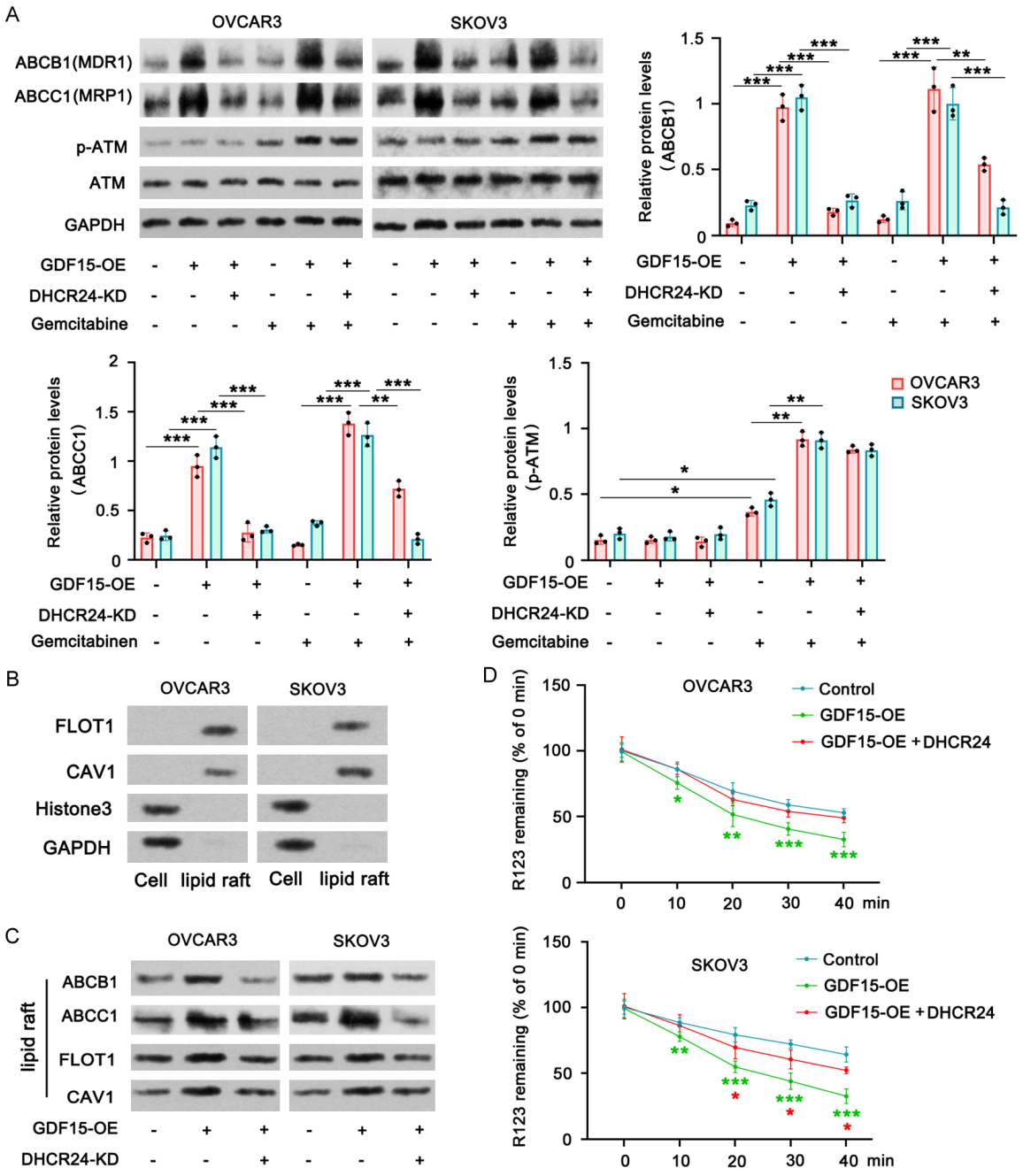

Figure 6. GDF15/DHCR24 increased ABCB1 and ABCC1 in the lipid raft to increase the the resistance of EOC to Gemcitabine. A. Western blot was conducted to detect ABCB1, ABCC1, p-ATM and ATM after GDF15 overexpression, DHCR24 knockdown and treatment with Gemcitabine. B. This study isolated lipid raft from the EOC. FLOT1 and CAV1 are proteins located in lipid raft. As shown in western blot, FLOT1 and CAV1 are in the isolated lipid raft, but not in the rest cell components. Histone3 and GAPDH were not detected in the isolated lipid raft. C. Western blot was conducted to detect ABCB1, ABCC1, FLOT1 and CAV1 in the isolated lipid raft. D. R123 level in cells was tested at various time points. Data expressed as mean ± standard deviation. *P*-value <0.05 was defined as specific statistical significance (*P<0.05, **P<0.01, ***P<0.001).

raft. GDF15 overexpression increased ABCB1 and ABCC1 expression in the isolated lipid raft, whereas DHCR24 knockdown suppressed the increase in ABCB1 and ABCC1 expression in the isolated lipid raft (**Figure 6C**). To further determine whether the functions of ABCB1 and

ABCC1 were regulated by GDF15 and DHCR24, we measured R123 levels in cells at various time points. GDF15 overexpression accelerated the reduction of R123 in cells, suggesting that GDF15 enhanced the ability of ABCB1 and ABCC1 to transport R123 outside cells (**Figure 6D**). DHCR24 knockdown suppressed the function of GDF15.

GDF15/DHCR24 increased the resistance of EOC cells to gemcitabine in xenograft tumors, which cannot be suppressed by statins

In the nude mouse xenograft tumor model, the tumor volume of EOC cells was increased by GDF15 overexpression; however, DHCR24 knockdown suppressed the function of GDF15 (**Figure 7A-C**). Although statins have been shown to decrease serum cholesterol levels [16], they have not been shown to increase tumor volume upon GDF15 overexpression. Treatment with gemcitabine strikingly suppressed the tumor volume, but GDF15 overexpression suppressed the effect of gemcitabine. DHCR24 knockdown, but not statin treatment, inhibited the function of GDF15 and counteracted gemcitabine toxicity. This study assessed GDF15 secretion levels in the tumor interstitial fluid. GDF15 overexpression promoted the secretion of GDF15, which was not affected by statins or DHCR24 knockdown (**Figure 7D**). Western blot analysis indicated that GDF15 overexpression increased the protein levels of DHCR24, ABCB1, and ABCC1 (**Figure 7E**). DHCR24 knockdown suppressed the increase in the levels of these three proteins; however, statins did not have such an effect.

Discussion

Previous studies have found abnormal GDF15 expression in ovarian cancer [10, 11]. Increased GDF15 expression promotes the proliferation and invasion of ovarian cancer cells. This study further found that GDF15 is involved in the reprogramming of glucose and cholesterol metabolism in EOC cells. Cholesterol metabolism regulated by GDF15 contributes to the resistance of EOC cells to gemcitabine by elevating ABCB1 and ABCC1 levels in lipid rafts. GDF15 exerts its biological functions mostly by interacting with the receptor GFRAL [17]. When GDF15 binds to GFRAL, RET, a key tyrosine kinase receptor, is recruited to the GDF15/GFRAL complex and is subsequently activated [17, 18]. This activation process involves the self-phosphorylation of RET. RET can further activate various cancer-promoting signaling pathways, such as PI3K/AKT, MAPK, and PLCγ [17, 18]. However, the downstream effectors that mediate the specific functions of GDF15 in EOC cells have not yet been fully elucidated.

This study revealed, for the first time, that DHCR24 is a novel downstream effector of GDF15. GDF15 overexpression increased DHCR24 expression in EOC cells. More importantly, DHCR24 knockdown abolished most of the functions of GDF15 in the regulation of cell viability, migration, and gemcitabine resistance. DHCR24 is a dehydrocholesterol reductase that plays a crucial role in cholesterol synthesis [19]. In recent years, an increasing number of studies have confirmed the important role of DHCR24 in various tumors, suggesting that it is a novel therapeutic target [20-22]. For example, one study found that the expression of DHCR24 is significantly increased in HER2-positive breast cancer tissues. DHCR24 facilitates the activation of the Hedgehog signaling pathway and increases the number of breast cancer stem cell-like cells [23]. DHCR24 also plays an important role in the development of hepatocellular carcinoma. Research has shown that high DHCR24 expression in HCC samples is associated with a poor clinical prognosis. Interference with DHCR24 suppresses the growth and migration of HCC cells. In addition, the natural product, genkwadaphnin, inhibits the expression and activity of DHCR24, which blocks cholesterol biosynthesis and lipid raft formation, consequently inhibiting the invasion and migration of HCC cells [24].

GDF15 regulates cholesterol metabolism mainly through DHCR24. In addition to DHCR24, this study found that GDF15 can regulate the expression of NPC1 and NPC2, both of which participate in the uptake of cholesterol from outside cells [25]. However, the regulatory effect of GDF15 on NPC1 and NPC2 was much weaker than that on DHCR24. This result suggests that the GDF15-induced increase in cholesterol levels in EOC cells is mainly dependent on cholesterol biosynthesis by DHCR24, rather than on the uptake of cholesterol by NPC1 and NPC2. Indeed, DHCR24 knockdown abolished most of the increase in cholesterol levels

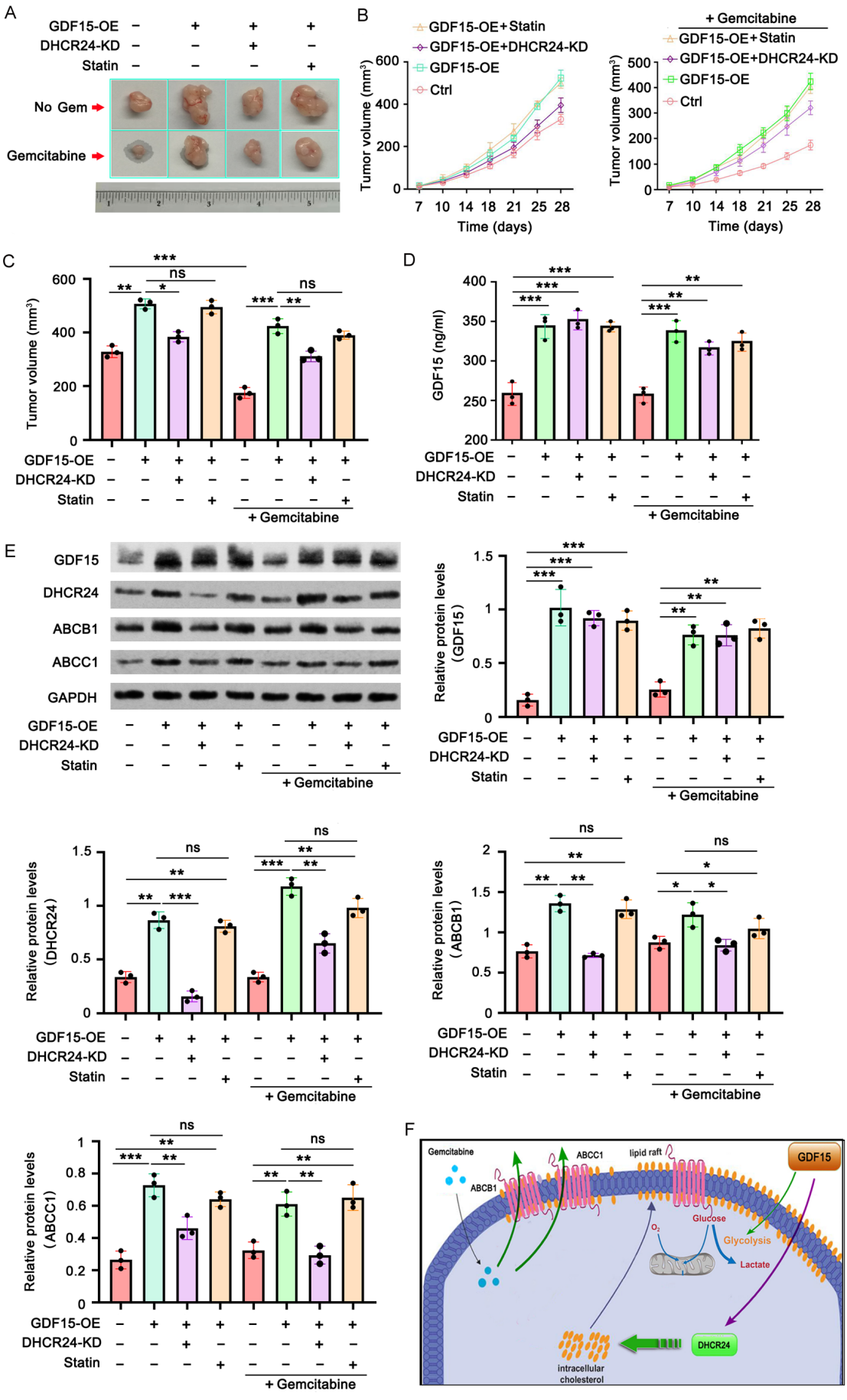
A
GDF15-OE
DHCR24-KD
Statin
No Gem
Gemcitabine
B
GDF15-OE+Statin
GDF15-OE+DHCR24-KD
GDF15-OE
Ctrl
Tumor volume (mm³)
Time (days)
+ Gemcitabine
C
Tumor volume (mm³)
D
GDF15 (ng/ml)
E
GDF15
DHCR24
ABCB1
ABCC1
GAPDH
Relative protein levels (GDF15)
Relative protein levels (DHCR24)
Relative protein levels (ABCB1)
Relative protein levels (ABCC1)
F
Gemcitabine
ABCB1
ABCC1
lipid raft
GDF15
Glucose
Glycolysis
Lactate
DHCR24
intracellular cholesterol

Figure 7. GDF15/DHCR24 increased the the resistance of EOC to Gemcitabine in xenograft tumors, which cannot be suppressed by Statin. A. A total of twenty-four female BALB/c nude mice (aged 4-6 weeks) were divided into eight groups, with three mice in each group. OVCAR3 cells in control and those with stable overexpression of GDF15 and stable knockdown of DHCR24 were injected subcutaneously into nude mice to construct a nude mouse tumor model. Nude mice with GDF15-overexpressed OVCAR3 cells were orally administered with mevastatin (500 mg/kg) every 2 days to inhibit cholesterol levels in the blood. A half of the mice were administered with gemcitabine (100 mg/kg) intraperitoneally once a week. Another half of the mice were administered with normal saline. B. The growth curve of tumor from day 7 to day 28. C. Tumor volume was calculated at day 28. D. This study assessed GDF15 secretion levels in the tumor interstitial fluid. GDF15 overexpression promoted the secretion of GDF15, which was not affected by Statin and DHCR24 knockdown. E. Western blot was conducted to detect GDF15, DHCR24, ABCB1 and ABCC1 in the xenograft tumors. F. The mechanism diagram of the role of GDF15 in the resistance of EOC to Gemcitabine. Data expressed as mean ± standard deviation. *P*-value <0.05 was defined as specific statistical significance (*P<0.05, **P<0.01, ***P<0.001).

induced by GDF15. Statins failed to suppress the cancer-promoting effects of GDF15. Statins, HMG-CoA reductase inhibitors, are capable of lowering serum cholesterol levels; therefore, they are commonly used to treat cardiovascular diseases. Recently, several reports have shown that statins inhibit the growth of various tumors, probably by hindering the production of cholesterol from the tumor microenvironment or cholesterol synthesis in cancer cells [26, 27]. However, other reports have indicated that statins have a weak effect on cancer progression and patient mortality and morbidity rates [28, 29]. One potential reason is that statins have different intracellular effects depending on their chemical structure [29], which may cause different outcomes during clinical treatment. Therefore, the effect of various types of statins on counteracting EOC with high GDF15 expression deserves further study.

Increased cholesterol levels in cancer cells has been associated with a strong resistance to chemical drugs [30, 31]. Cholesterol can be used to synthesize vitamin D3 and make up the cell membrane, especially the membrane lipid rafts. Lipid rafts contain high concentrations of cholesterol to maintain fluidity and perform other functions. Many proteins have been found to accumulate in lipid rafts, which maintains protein function, stabilizes certain proteins together, and influences protein turnover [6, 32]. ABCB1 and ABCC1 are partially located in lipid rafts, and their functions depend on their direct lipid environment. ABCB1 has a higher affinity for its substrates when the surrounding lipids are in the liquid-ordered phase rather than in the liquid-disordered phase [33, 34]. ABCB1 levels in lipid rafts are likely regulated by cholesterol. Troost et al. found that cholesterol depletion removes ABCB1 from raft membranes, resulting in the intracellular accumulation of ABCB1 [35]. Consequently, ABCB1 activity in the efflux substrate is reduced. However, cholesterol depletion restores ABCB1 activity. Yun et al. found that Rp1, a novel ginsenoside derivative, decreased ABCB1 activity in EOC cells, but the addition of cholesterol attenuated Rp1-induced raft aggregation and restored ABCB1 activity [14]. In our study, GDF15 overexpression increased the number of lipid rafts and ABCB1 and ABCC1 protein levels. Consistent with our results, Hu et al. used methyl-β-cyclodextrin to destroy the lipid raft structure on the HCC cell membrane, which notably attenuated ABCB1 levels on the cell membrane [36]. These results suggest that ABCB1 levels are influenced by the lipid raft structure. As indicated by the output of R123 from the cells, GDF15 also increased the functions of ABCB1 and ABCC1. ABCB1 and ABCC1 can release a wide range of drugs, particularly lipophilic and amphiphilic drugs. This characteristic of ABCB1 and ABCC1 may explain why overexpression of GDF15 enhanced cell resistance to lipophilic gemcitabine more effectively than to carboplatin, which has poor liposolubility.

Overall, this study found that GDF15 is involved in the reprogramming of glucose and cholesterol metabolism in EOC cells. The cholesterol metabolism regulated by GDF15 contributed to the resistance of EOC cells to gemcitabine by elevating ABCB1 and ABCC1 levels in lipid rafts. As a downstream effector of GDF15, DHCR24 plays an important role in cholesterol synthesis. A diagram of this mechanism is presented in **Figure 7F**. The results of this study suggest that GDF15 and DHCR24 are potential therapeutic targets to suppress the growth of EOC cells and improve their sensitivity to gemcitabine.

Acknowledgements

This study was funded by the Project of Liaoning Provincial Department of Education (LJKZ0810).

Disclosure of conflict of interest

None.

Address correspondence to: Yan He, Department of Laboratory, Animal Science, China Medical University, No. 77 Puhe Road, Shenyang North New Area, Shenyang 110122, Liaoning, PR China. E-mail: 20172165@cmu.edu.cn; Huang Xin, Department of Obstetrics and Gynecology, First Affiliated Hospital of Jinzhou Medical University, No. 2, Section 5, Renmin Street, Guta District, Jinzhou 121001, Liaoning, PR China. E-mail: 18874804163@163.com; guoll1@jzmu.edu.cn

References

[1] Wang Y, Wang Z, Zhang Z, Wang H, Peng J and Hong L. Burden of ovarian cancer in China from 1990 to 2030: a systematic analysis and comparison with the global level. Front Public Health 2023; 11: 1136596.

[2] Feng J, Xu L, Chen Y, Lin R, Li H and He H. Trends in incidence and mortality for ovarian cancer in China from 1990 to 2019 and its forecasted levels in 30 years. J Ovarian Res 2023; 16: 139.

[3] Nantasupha C, Thonusin C, Charoenkwan K, Chattipakorn S and Chattipakorn N. Metabolic reprogramming in epithelial ovarian cancer. Am J Transl Res 2021; 13: 9950-9973.

[4] Ayyagari VN, Wang X, Diaz-Sylvester PL, Groesch K and Brard L. Assessment of acyl-CoA cholesterol acyltransferase (ACAT-1) role in ovarian cancer progression-an in vitro study. PLoS One 2020; 15: e0228024.

[5] Liang Y, Nephew KP and Hyder SM. Cholesterol biosynthesis inhibitor RO 48-8071 suppresses growth of epithelial ovarian cancer cells in vitro and in vivo. J Cancer Sci Clin Ther 2023; 7: 1-8.

[6] Zhang S, Zhu N, Li HF, Gu J, Zhang CJ, Liao DF and Qin L. The lipid rafts in cancer stem cell: a target to eradicate cancer. Stem Cell Res Ther 2022; 13: 432.

[7] Nedeljković M, Tanić N, Prvanović M, Milovanović Z and Tanić N. Friend or foe: ABCG2, ABCC1 and ABCB1 expression in triple-negative breast cancer. Breast Cancer 2021; 28: 727-736.

[8] Mo J, Kang M, Ye JX, Chen JB, Zhang HB and Qing C. Gibberellin derivative GA-13315 sensitizes multidrug-resistant cancer cells by antagonizing ABCB1 while agonizes ABCC1. Cancer Chemother Pharmacol 2016; 78: 51-61.

[9] Li S, Ma YM, Zheng PS and Zhang P. GDF15 promotes the proliferation of cervical cancer cells by phosphorylating AKT1 and Erk1/2 through the receptor ErbB2. J Exp Clin Cancer Res 2018; 37: 80.

[10] Griner SE, Joshi JP and Nahta R. Growth differentiation factor 15 stimulates rapamycin-sensitive ovarian cancer cell growth and invasion. Biochem Pharmacol 2013; 85: 46-58.

[11] Guo LL and Wang SF. Downregulated long noncoding RNA GAS5 fails to function as decoy of CEBPB, resulting in increased GDF15 expression and rapid ovarian cancer cell proliferation. Cancer Biother Radiopharm 2019; 34: 537-546.

[12] Eil R, Vodnala SK, Clever D, Klebanoff CA, Sukumar M, Pan JH, Palmer DC, Gros A, Yamamoto TN, Patel SJ, Guittard GC, Yu Z, Carbonaro V, Okkenhaug K, Schrump DS, Linehan WM, Roychoudhuri R and Restifo NP. Ionic immune suppression within the tumour microenvironment limits T cell effector function. Nature 2016; 537: 539-543.

[13] Xie B, Tang W, Wen S, Chen F, Yang C, Wang M, Yang Y and Liang W. GDF-15 inhibits ADP-induced human platelet aggregation through the GFRAL/RET signaling complex. Biomolecules 2023; 14: 38.

[14] Yun UJ, Lee JH, Koo KH, Ye SK, Kim SY, Lee CH and Kim YN. Lipid raft modulation by Rp1 reverses multidrug resistance via inactivating MDR-1 and Src inhibition. Biochem Pharmacol 2013; 85: 1441-1453.

[15] da Costa KM, Freire-de-Lima L, da Fonseca LM, Previato JO, Mendonça-Previato L and Valente RDC. ABCB1 and ABCC1 function during TGF-beta-induced epithelial-mesenchymal transition: relationship between multidrug resistance and tumor progression. Int J Mol Sci 2023; 24: 6046.

[16] Murto MO, Simolin N, Arponen O, Siltari A, Artama M, Visvanathan K, Jukkola A and Murtola TJ. Statin use, cholesterol level, and mortality among females with breast cancer. JAMA Netw Open 2023; 6: e2343861.

[17] Buchholz K, Antosik P, Grzanka D, Gagat M, Smolińska M, Grzanka A, Gzil A, Kasperska A and Klimaszewska-Wiśniewska A. Expression of the body-weight signaling players: GDF15, GFRAL and RET and their clinical relevance in gastric cancer. J Cancer 2021; 12: 4698-4709.

[18] Zhao Z, Zhang J, Yin L, Yang J, Zheng Y, Zhang M, Ni B and Wang H. Upregulated GDF-15 expression facilitates pancreatic ductal adenocarcinoma progression through orphan recep-

tor GFRAL. Aging (Albany NY) 2020; 12: 22564-22581.
[19] Müller C, Hank E, Giera M and Bracher F. Dehydrocholesterol reductase 24 (DHCR24): medicinal chemistry, pharmacology and novel therapeutic options. Curr Med Chem 2022; 29: 4005-4025.
[20] Shen Y, Zhou J, Nie K, Cheng S, Chen Z, Wang W, Wei W, Jiang D, Peng Z, Ren Y, Zhang Y, Fan Q, Richards KL, Qi Y, Cheng J, Tam W and Ma J. Oncogenic role of the SOX9-DHCR24-cholesterol biosynthesis axis in IGH-BCL2+ diffuse large B-cell lymphomas. Blood 2022; 139: 73-86.
[21] Yan L, Wu X, Zhang Y, Tan Q, Xu J, Wang Y, Wang R, Li Y and Zhao J. LncRNA ENST-00000370438 promotes cell proliferation by upregulating DHCR24 in breast cancer. Mol Carcinog 2023; 62: 855-865.
[22] Zhang Y, Wang M, Meng F, Yang M, Chen Y, Guo X, Wang W, Zhu Y, Guo Y, Feng C, Tian S, Zhang H, Li H, Sun J and Wang W. A novel SRSF3 inhibitor, SFI003, exerts anticancer activity against colorectal cancer by modulating the SRSF3/DHCR24/ROS axis. Cell Death Discov 2022; 8: 238.
[23] Qiu T, Cao J, Chen W, Wang J, Wang Y, Zhao L, Liu M, He L, Wu G, Li H and Gu H. 24-dehydrocholesterol reductase promotes the growth of breast cancer stem-like cells through the Hedgehog pathway. Cancer Sci 2020; 111: 3653-3664.
[24] Wu J, Guo L, Qiu X, Ren Y, Li F, Cui W and Song S. Genkwadaphnin inhibits growth and invasion in hepatocellular carcinoma by blocking DHCR24-mediated cholesterol biosynthesis and lipid rafts formation. Br J Cancer 2020; 123: 1673-1685.
[25] Prakash S, Saini S, Kumari S, Singh B, Kureel AK and Rai AK. Retinoic acid restores the levels of cellular cholesterol in Leishmania donovani infected macrophages by increasing npc1 and npc2 expressions. Biochimie 2022; 198: 23-32.
[26] Beckwitt CH, Brufsky A, Oltvai ZN and Wells A. Statin drugs to reduce breast cancer recurrence and mortality. Breast Cancer Res 2018; 20: 144.
[27] Alfaqih MA, Allott EH, Hamilton RJ, Freeman MR and Freedland SJ. The current evidence on statin use and prostate cancer prevention: are we there yet? Nat Rev Urol 2017; 14: 107-119.
[28] Liu B, Yi Z, Guan X, Zeng YX and Ma F. The relationship between statins and breast cancer prognosis varies by statin type and exposure time: a meta-analysis. Breast Cancer Res Treat 2017; 164: 1-11.
[29] Jiang W, Hu JW, He XR, Jin WL and He XY. Statins: a repurposed drug to fight cancer. J Exp Clin Cancer Res 2021; 40: 241.
[30] Wang Y, Cai L, Li H, Chen H, Yang T, Tan Y, Guo Z and Wang X. Overcoming cancer resistance to platinum drugs by inhibiting cholesterol metabolism. Angew Chem Int Ed Engl 2023; 62: e202309043.
[31] Sheng N, Wang YQ, Wang CF, Jia MQ, Niu HM, Lu QQ, Wang YN, Feng D, Zheng XX and Yuan HQ. AGR2-induced cholesterol synthesis drives lovastatin resistance that is overcome by combination therapy with allicin. Acta Pharmacol Sin 2022; 43: 2905-2916.
[32] Sonnino S, Aureli M, Grassi S, Mauri L, Prioni S and Prinetti A. Lipid rafts in neurodegeneration and neuroprotection. Mol Neurobiol 2014; 50: 130-148.
[33] Hummel I, Klappe K, Ercan C and Kok JW. Multidrug resistance-related protein 1 (MRP1) function and localization depend on cortical actin. Mol Pharmacol 2011; 79: 229-40.
[34] Meszaros P, Hummel I, Klappe K, Draghiciu O, Hoekstra D and Kok JW. The function of the ATP-binding cassette (ABC) transporter ABCB1 is not susceptible to actin disruption. Biochim Biophys Acta 2013; 1828: 340-351.
[35] Troost J, Lindenmaier H, Haefeli WE and Weiss J. Modulation of cellular cholesterol alters P-glycoprotein activity in multidrug-resistant cells. Mol Pharmacol 2004; 66: 1332-9.
[36] Hu B, Zou T, Qin W, Shen X, Su Y, Li J, Chen Y, Zhang Z, Sun H, Zheng Y, Wang CQ, Wang Z, Li TE, Wang S, Zhu L, Wang X, Fu Y, Ren X, Dong Q and Qin LX. Inhibition of EGFR overcomes acquired lenvatinib resistance driven by STAT3-ABCB1 signaling in hepatocellular carcinoma. Cancer Res 2022; 82: 3845-3857.

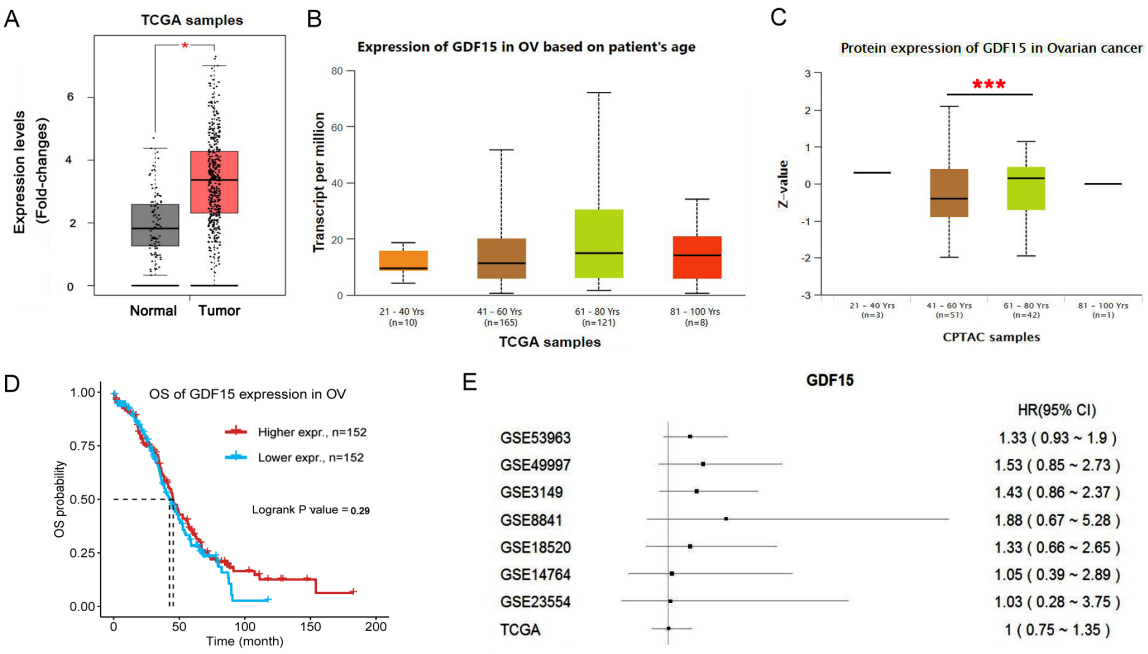

F

Dataset	Variables	Univariate analysis			Multivariate analysis			Outcome
		p value	HR	95% CI	p value	HR	95% CI	Uni/Multi-variable
GSE26193	GDF15	0.1535	0.66	0.38~1.17	0.6159	0.92	0.68~1.26	-/-
	Stage	<0.0001	2.06	1.55~2.74	<0.0001	2.07	1.75~2.44	Poor/Poor
GSE30161	GDF15	0.1723	0.54	0.22~1.31	0.6012	0.89	0.56~1.40	-/-
	race	0.0989	2.44	0.85~7.06	0.0047	2.44	1.31~4.51	-/Poor
GSE32063	GDF15	0.5412	0.71	0.24~2.13	0.2793	0.52	0.16~1.69	-/-
	grade	0.1940	1.78	0.75~4.24	0.0684	2.47	0.93~6.51	-/-
	Stage	0.1240	2.15	0.81~5.72	0.0375	3.16	1.07~9.32	-/Poor
GSE49997	GDF15	0.1529	1.53	0.85~2.73	0.1151	1.61	0.89~2.93	-/-
	age	0.0172	1.89	1.12~3.19	0.0360	1.78	1.04~3.04	Poor/Poor
	grade	0.0324	0.46	0.22~0.94	0.0393	0.47	0.23~0.96	Good/Good
	Stage	0.0280	1.90	1.07~3.36	0.1388	1.55	0.87~2.77	Poor/-
GSE51088	GDF15	0.4960	0.86	0.55~1.34	0.6894	1.10	0.68~1.80	-/-
	age	0.1760	1.16	0.94~1.44	0.0003	2.07	1.39~3.08	-/Poor
	histology	<0.0001	2.21	1.50~3.24	0.7473	0.96	0.74~1.24	Poor/-
	Stage	0.0002	1.73	1.29~2.30	0.0023	1.73	1.22~2.45	Poor/Poor
GSE53963	GDF15	0.1236	1.33	0.93~1.90	0.1472	1.31	0.91~1.88	-/-
	age	0.1900	1.24	0.90~1.70	0.3860	1.15	0.84~1.59	-/-
	Stage	0.0003	1.80	1.31~2.48	0.0006	1.77	1.28~2.46	Poor/Poor
GSE63885	GDF15	0.2183	0.70	0.39~1.24	0.9281	0.99	0.71~1.36	-/-
	grade	0.0113	1.71	1.13~2.58	<0.0001	1.66	1.30~2.12	Poor/Poor
	Stage	0.0084	2.31	1.24~4.32	<0.0001	2.20	1.52~3.17	Poor/Poor
GSE73614	GDF15	0.9371	0.98	0.52~1.82	0.5657	1.21	0.63~2.34	-/-
	age	0.0275	1.79	1.07~2.99	0.1352	1.50	0.88~2.55	Poor/-
	grade	0.0068	1.84	1.18~2.85	0.1301	1.44	0.90~2.30	Poor/-
	Stage	0.0001	1.73	1.30~2.30	0.0023	1.59	1.18~2.14	Poor/Poor
GSE8841	GDF15	0.2334	1.88	0.67~5.28	0.9850	0.99	0.29~3.37	-/-
	age	0.0639	3.02	0.94~9.74	0.9076	1.10	0.22~5.52	-/-
	grade	0.0507	2.39	1.00~5.73	0.1312	2.03	0.81~5.08	-/-
	Histotype	0.0364	0.60	0.37~0.97	0.2146	0.73	0.45~1.20	Good/-
GSE9891	GDF15	0.4678	0.83	0.50~1.38	0.5104	1.09	0.84~1.43	-/-
	age	0.1090	1.43	0.92~2.22	0.0227	1.34	1.04~1.73	-/Poor
	Histological	0.0372	8.14	1.13~58.48	0.0048	5.18	1.65~16.26	Poor/Poor
	Stage	<0.0001	2.41	1.60~3.61	<0.0001	2.21	1.74~2.82	Poor/Poor
TCGA	GDF15	0.9907	1.00	0.75~1.35	0.6471	0.93	0.68~1.27	-/-
	age	<0.0001	1.56	1.26~1.94	0.0078	1.46	1.10~1.92	Poor/Poor
	grade	0.1680	1.23	0.92~1.64	0.5341	1.14	0.75~1.72	-/-
	race	0.0986	0.81	0.63~1.04	0.0087	0.66	0.49~0.90	-/Good
	Stage	0.0008	1.43	1.16~1.76	0.0782	1.31	0.97~1.77	Poor/-

Supplementary Figure 1. Bioinformatics analysis of GDF15 expression and its association with the overall survival in ovarian cancer. A. The mRNA expression level of GDF15 was analyzed in ovarian cancer and corresponding normal tissues using the data in database TCGA. GDF15 expression is up-regulated in ovarian cancer in comparison to the corresponding normal tissues. B. As indicated by TCGA, GDF15 mRNA expression is marginally increased in patients with ovarian cancer at 61-80 years old compared to patients at other age stages. C. UALCAN provides protein

expression analysis using data from Clinical Proteomic Tumor Analysis Consortium (CPTAC) and the International Cancer Proteogenome Consortium (ICPC) datasets. Data from UALCAN that show that GDF15 protein level is significantly increased in patients with ovarian cancer at 61-80 years old compared to patients at 40-60 years old. D. As indicated by TCGA database, GDF15 expression level is not related to the prognosis of patients with ovarian cancer. E. The association of GDF15 expression to overall survival of the patient with ovarian cancer was analyzed by Hazard Ratio (HR) using OSov, a public web for bioinformatics analysis. OSov shows that GDF15 expression is related to the overall survival of patients with ovarian cancer according to data from GSE53963, GSE49997, GSE3149, GSE8841 and GSE18520 datasets. F. The age, stage, histology and grade, but not GDF15 expression, are related to the overall survival of patients with ovarian cancer in several univariate and multivariate analysis, using data in GSE51088, GSE73614 and GSE9891 datasets.

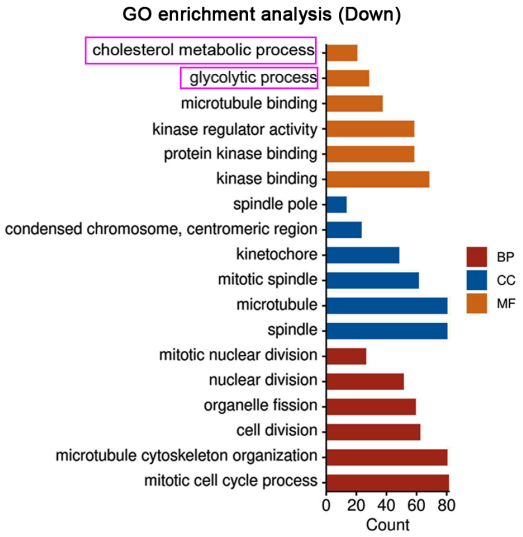

Supplementary Figure 2. GO-enrichment analysis of biological processes regulated by GDF15. The high-throughput sequencing assay showed that many genes were impacted by GDF15 knockdown. The down-regulated genes were used for GO-enrichment analysis to find which biological processes are regulated by GDF15. The analysis implied that metabolisms, such as cholesterol and glycolysis, are regulated by GDF15.

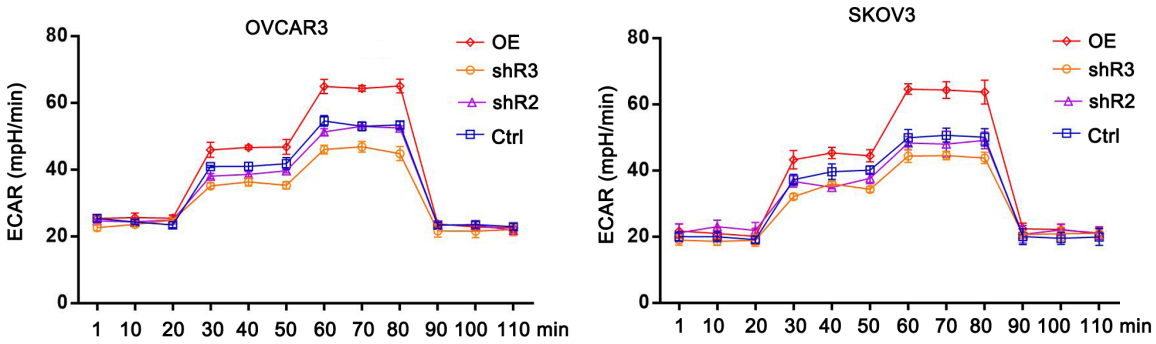

Supplementary Figure 3. ECAR tests to assess the lactic acid secreted by EOC. This study also tested the ECAR to assess the lactic acid secreted by EOC. GDF15 knockdown decreased the ECAR, while GDF15 overexpression increased the ECAR.